

## **n\_TOF: TIMEPIX-BASED DIAGNOSTIC SYSTEMS FOR NEUTRONS DETECTION, CROSS SECTION MEASUREMENTS AND BNCT**

G. Claps<sup>1,2</sup> (Resp.), N. Terranova<sup>1,2</sup> (Ass.), A. Pietropaolo<sup>1,2</sup> (Ass.),  
L. Foggetta<sup>1</sup>, D. Tagnani<sup>1</sup> (Tecn.), A. Tamburrino (Dott.), S. Tosi (Dott.)

*1 - INFN – Laboratori Nazionali di Frascati, via E. Fermi 54, 00044 Frascati, Italy*

*2 - ENEA FSN Department, C. R. Frascati, via E. Fermi 45, 00044 Frascati, Italy*

*Collaborations: CERN-European Organization for Nuclear Research (Switzerland), CNR-ISTP (Milano), Università Milano Bicocca, LENA-Laboratorio Energia Nucleare Applicata (Pavia)*

### **1 Introduction**

Our activity during the last year falls in the framework of a collaboration between ENEA and INFN in Frascati and follows two main research lines: the development of a new diagnostic system based on GEMPix and Timepix detectors for neutron cross section measurements and the characterization of new timepix-based detectors for neutrons and charged particles detection. These activities found their physical interest in the field of nuclear fusion, radio-protection, medical applications and nuclear astrophysics, as will be explained in the next sections. After a brief introduction to the n\_TOF facility and the main neutron sources used by our group, the report will focus on three main results obtained in the last year: the characterization of the new diamond detector based on Timepix3 (TPX3) for fast neutrons and a CdTe TPX3 detector with LiF converter for thermal neutrons, the measurements and identification of charged products with GEMPix detector on a Carbon target and measurements of Boron distribution on silicon samples of interest for Boron Neutron Capture Therapy (BNCT).

### **2 Neutron Facilities**

In the framework of the n\_TOF collaboration, our group actively participates both as support and as facility users. The n\_TOF plant at CERN is a neutron spallation source and hosts a series of experiments dedicated to various applications relevant to basic nuclear physics, astrophysics, nuclear medicine and emerging nuclear technology: measurements of capture sections on radioactive samples, long-life fission fragments, capture and fission sections of minor actinides, necessary for nuclear waste transmutation projects and for the design of innovative nuclear systems, such as accelerator systems and fourth-generation fast nuclear reactors. n\_TOF has two neutron beam lines with two measuring stations; in the first called EAR1 the beam arrives after traveling along a flight path of 185 m with a high instantaneous flux. In EAR1, the time of flight technique allows for measuring neutron energy over a wide range with good resolution. At 12 m from the EAR1 station, there is the beam dump area that is often used for testing new detectors. In the second

measuring station, called EAR2, the beam arrives after a trajectory of 19 m with a higher neutron flux in the position of the sample with respect to EAR1. The EAR2 station is dedicated to the study of short-lived isotopes. Neutron sources where our experiments are often conducted are FNG (Frascati Neutron Generator) and HOTNES at the ENEA Frascati research center. FNG is a neutron generator based on an electrostatic accelerator and produces 14.0 MeV and 2.5 MeV neutrons using the fusion reactions  $T(d,n)\alpha$  and  $D(d,n)^3\text{He}$ , respectively. Neutron emission is isotropic and can reach an emission rate up to  $10^{11}$  n/s. HOTNES is a passive neutron source based on moderated sealed neutron source AmB. The source of AmB has been incorporated in a polyethylene structure in order to obtain a uniform flux of thermal neutrons on circular planes of 30 cm in diameter with a peak energy of 25 meV. The main plane is localized 50 cm from the AmB source with a neutron flux of  $763$  n/cm<sup>2</sup>/s.

### 3 Timepix3-based detectors for fast neutrons and thermal neutrons

Neutron diagnostic provides many important parameters on fusion reactors: fusion reaction rates, fuel ion temperature and density, beam plasma interaction and the evaluation of neutron load on components due to vacuum chamber and divertor. In this framework, our group developed a new diamond detector based on a Timepix3 chip for the expected fast neutron spectrum (1- 20 MeV). For the thermal neutron component, instead, a CdTe TPX3 equipped with a LiF converter has been realized and characterized.

#### 3.1 The Diamondpix detector for fast neutrons

As is known, diamond is a radiation hard material and represents an excellent candidate in high radiation flux environments like those expected on modern fusion reactors. At the moment, our group is working on a new diamond detector realized by a coupling of a diamond plate to a TPX3 chip [1]: the "Diamondpix" [2]. Our first prototype is based on CVD diamond  $500\ \mu\text{m}$  in thickness and with an area of  $10 \times 10\ \text{mm}^2$ . On one side, a matrix of small conductive pads has been deposited in order to realize a coupling to the TPX3 chip through the bump-bonding technique. On the other side, a 300 nm Gold layer has been deposited in order to obtain the polarization electrode. As a result, the Diamondpix is a 2D diamond detector with an area of about  $1\ \text{cm}^2$  and pixels of  $55 \times 55\ \mu\text{m}^2$  as for standard semiconductor TPX3 detectors. In addition, with respect to Timepix1, the Timepix3 chip can acquire simultaneously in counting, ToT and ToA modes and can reach time resolution down to 1.6 ns. Diamondpix has been characterized on the n-TOF facility by means of time-of-flight (tof) measurements. In this way, it was possible to select specific energies by means of tof measurements and study their response in terms of track morphology and charge. Diamondpix was installed in the dump area after the EAR1 experimental area at a distance of 197 m from the target where the neutron beam is produced. Measurements were performed during the 2022 n\_TOF run and data analysis was completed in 2023, subject of the PhD thesis work of A. Tamburrino [3] where we refer for further details. Interaction of a neutron in the diamond produces a cluster of pixels, i.e. a 2D track, having a specific morphology and charge. Then, applying appropriate cuts on defined morphological parameters and selecting specific ranges of the

released energies, it is possible to identify the tracks due to neutrons and discard those arising from the interaction of other particles, particularly the gamma background (fig. 1).

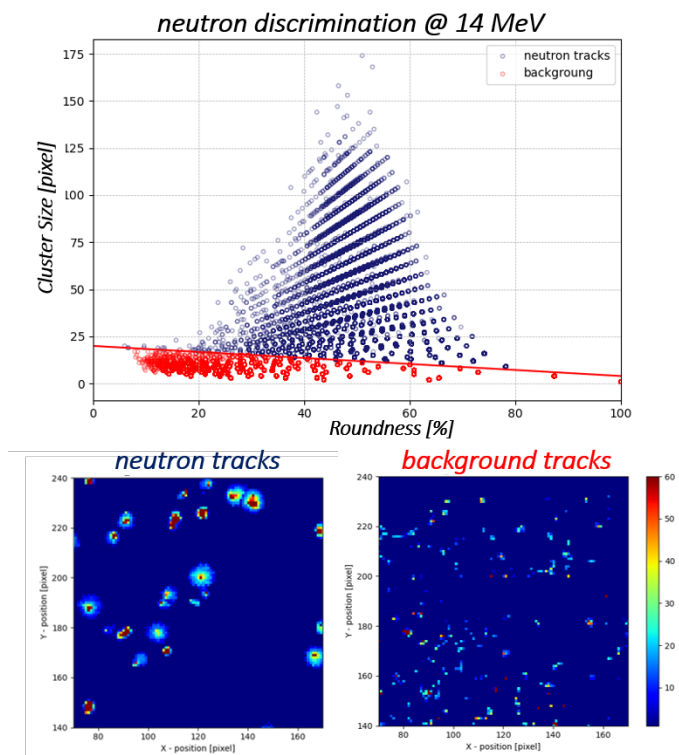


Figure 1: *Particle tracks observed on Diamondpix: blue circles highlight the tracks from neutron interactions, red circles those from gamma interactions; in the lower half the tracks as they appear in the neutron and gamma regions.*

After the discrimination of neutron tracks, the corresponding ToA measures allowed to get the neutron spectrum of the n-TOF neutron beam (fig. 2). As expected, it can be observed that for energies less than 1 MeV, there are no signals because no significant reactions can be exploited for lower energy neutrons and the detector threshold cuts lower charges. Fig. 2 also outlines some clear resonance peaks characteristic of the Carbon cross-section.

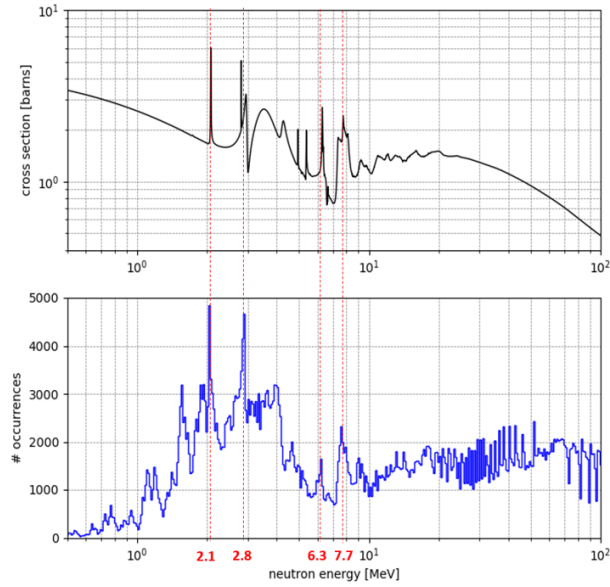


Figure 2: *n-TOF* neutron spectrum as reconstructed with *Diamondpix* in time of flight; comparison with the total Carbon cross section shows some characteristic peaks in accordance with resonances.

The obtained tof spectrum has been used to identify some specific energies to calibrate the detector. In order to exploit only the contribution from the recoil of carbon ions and avoid the other Carbon characteristic reactions, a set of discrete neutron energies from 1 to 5.7 MeV was selected and used for calibration. In particular, the maximum released charge (in ToT units) was correlated to the maximum Carbon ion recoil energy (fig. 3).

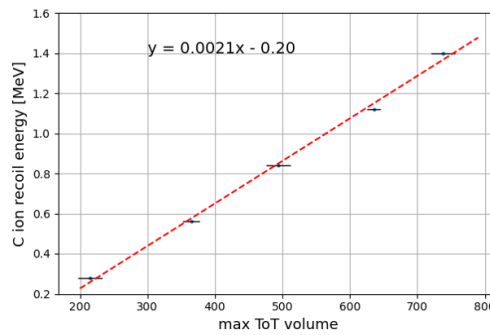


Figure 3: *Energy calibration curve* as obtained from the maximum *ToT* values due to Carbon ion recoils from neutrons at energies from 1 to 5 MeV with a step of 1 MeV.

Then the obtained calibration curve was useful for the identification of the characteristic diamond reactions at higher energies, in particular  $^{12}\text{C}(n,3\alpha)$  and  $^{12}\text{C}(n,\alpha)^9\text{Be}$ . Analysis of neutron energies higher than 5.7 MeV shows the presence of tracks due to the contribution of these reactions but cannot be clearly identified. In particular, the expected peak coming from the  $^{12}\text{C}(n,\alpha)$  reaction was not observed. These results were expected because the diamond used for this prototype was

poly-crystalline and charge transport in 500  $\mu\text{m}$  of material is limited as outlined by the low value of charge collection distance (only 300  $\mu\text{m}$ ). This type of diamond was used to demonstrate the feasibility of this new detector and evaluate its performance as 2D detector. The next step will be the realization of a Diamondpix with a mono-crystalline diamond in order to improve also charge measurements. For further details, we refer to the PhD thesis of A. Tamburrino [3].

#### 4 CdTe Timepix3 with LiF converter for thermal neutrons

For the monitor of thermal neutrons, our group developed a CdTe TPX3 equipped with a Silicon sheet deposited with 5  $\mu\text{m}$  LiF layer enriched with  $^6\text{Li}$  in order to detect neutrons through  $^6\text{Li}(\alpha,n)^3\text{He}$  reaction. This TPX3 detector has been equipped with an Aluminum mask supporting the Silicon sheet with LiF that covers one-half of the sensitive surface (fig.4a). The converter layer is separated by 3 mm from the TPX3 surface (fig 4b).

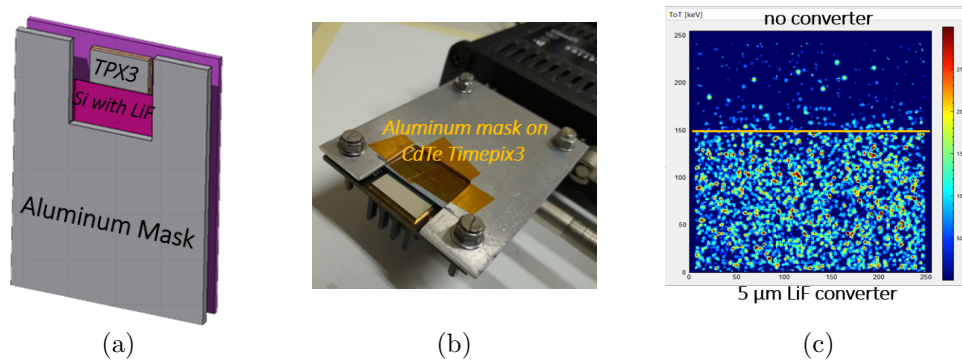


Figure 4: a) Layout of the CdTe Timepix3 detector with Al mask and Silicon sheet with LiF converter; b) a photo of the experimental TPX3 set-up; c) tracks on CdTe Timepix3 surface, most of them fall in correspondence of the area covered by LiF converter.

This layout was useful because allowed us to evaluate the effect of the LiF converter. First tests have been performed at the HOTTNES facility, then with neutrons peaked at 25 meV. The obtained results are satisfying as can be observed in fig. 4c. In addition, track analysis allowed to discriminate the contributions due to  $\alpha$  and tritons. This can be particularly observed in the energy distribution histograms that show the presence of two populations: a lower one due to alpha particles and a higher one due to tritons (fig. 5a). These distributions have been also confirmed from MC simulation (fig. 5b).

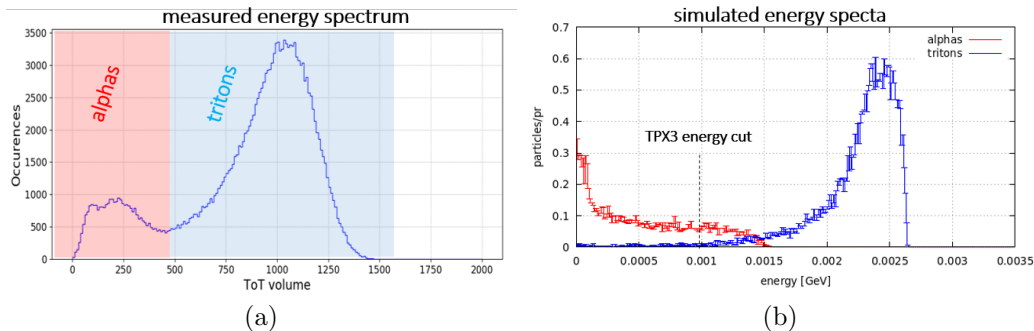


Figure 5: *a) ToT volume distribution after alphas and tritons tracks identification: it is possible to distinguish the two contributions; b) Fluka simulation of the alpha and triton spectra reaching the detector surface, it is clear the main contribution of tritons;*

Selecting the contributions coming from the two reaction products, the measured efficiency with 5  $\mu\text{m}$  LiF converter was about 0.9%, as expected. For further details, we refer to the publication of A. Tamburrino. Previous works [4] demonstrated that the optimal LiF layer thickness to obtain the maximum efficiency for 25 meV neutrons should be 25  $\mu\text{m}$ .

## 5 GEMpix detector for measurements of charged reaction products

In the framework of the n-TOF collaboration, the activity proposed by the ENEA/LNF group is in the field of nuclear fusion and focalizes on the effects of radiation damage on structural materials constituting the inner part of Tokamaks, especially in the blanket and divertor which are subjected to extremely high neutron fluxes. Particularly important are the reactions (n, cp), that is reactions with production of light charged particles such as protons, deuterons, tritium and alpha particles, responsible for the production of hydrogen and helium. The presence of these elements determines a change in the thermo-mechanical bonds of the structural elements and a consequent embrittlement of the structures [5]. The study of neutron cross sections for some materials has important implications in other fields like nuclear astrophysics and medical physics. (n, cp) reactions characterize many processes that take place inside stars. Among the most important reactions we mention those that produce protons for the subsequent  $^{14}\text{N}(n, p)^{14}\text{C}$  reaction useful for helium-shell burning [6] and reactions producing  $^7\text{Li}$ . In this second case, there is a discrepancy between models and measured data, and it is necessary to study also the (n,  $\alpha$ ) and (n, p) channels [7]. In nuclear medicine, there are also implications in several fields like dosimetry, neutron therapy and isotopes production. A specific application in this field is the object of the next paragraph. Within this research program, the ENEA/LNF group has developed a new GEMpix detector [8] configured to observe charged products coming from (n, cp) reactions. Due to some technical problems, however, the planned configuration for the first experimental campaign on the n-TOF facility was different. The proposed GEMpix has a standard configuration: a triple GEM camera read by a Timepix1 quad (fig. 6a). The experiment was aimed to study the reaction products coming from a carbon target. In this case, a sheet of graphite was used and located on the entrance window of the GEMpix (fig. 6b).

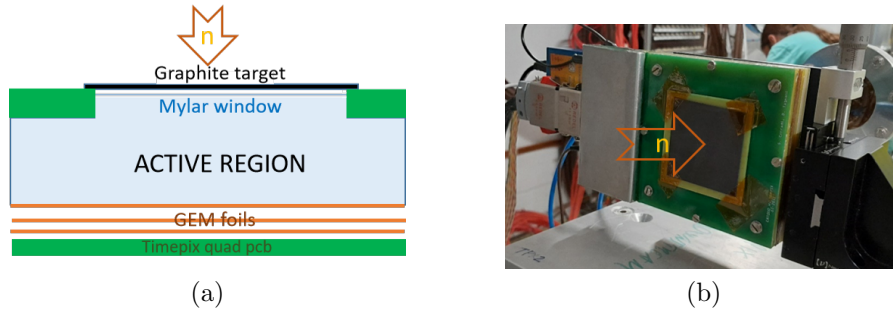


Figure 6: a) Layout of the the GEMpix detector with the graphite target placed before the mylar window; b) a photo of the GEMpix detector with graphite target installed in the  $n$ -TOF EAR1.

As demonstrated by subsequent MC simulations, the measure of charged products coming from the Target is severely limited by the GEMpix entrance window. It is made of a  $15\ \mu\text{m}$  Aluminated Mylar that stops many of the produced charged particles. However, the capability of this detector to identify different types of particles was tested with those produced by neutron interaction on Mylar itself. As explained in a dedicated publication, the GEMpix is read by a Timepix1 chip quad and this read-out electronics can acquire in counting, charge or time in a defined time window [9]. In order to measure the energy tracks, measurements have been performed in charge mode in a time window short enough to avoid tracks overlap. In addition time window cannot be too short because ToT measures could be limited. Then, taking into account these opposing advantages, the time window was set to a minimum of  $100\ \mu\text{s}$ . Then, applying appropriate trigger delays, different energy windows were investigated. Some of the most interesting results were obtained in the energy range from 1 MeV to 10 keV (fig. 7a).

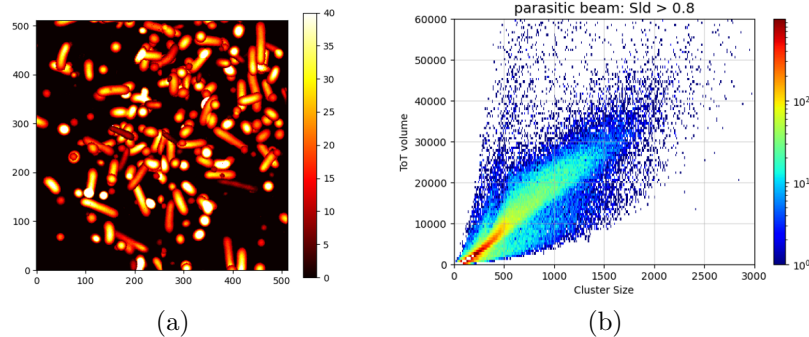


Figure 7: a) All types of tracks acquired in 10 triggers, each with a frame time window of  $100\ \mu\text{s}$ ; b) 2D histogram plot of the ToT volume versus Cluster Size for an acquisition of  $10^4$  triggers.

The particle detected in the active gas volume of GEMpix are observed as cluster of pixels, a group of adjacent pixels composing the track. Once defined the solidity (sld) parameter to discard overlapped tracks, an 2D histogram of the ToT volume (the sum of all pixel ToT values belonging to the cluster) versus Cluster Size (the sum of all pixels of the cluster) shows some populations (fig. 7b). Defining the Roundness (Rnd) parameter as the ratio between the Cluster Size and the area of a circumference containing the cluster, it is possible to distinguish two main populations as shown in fig. 8.

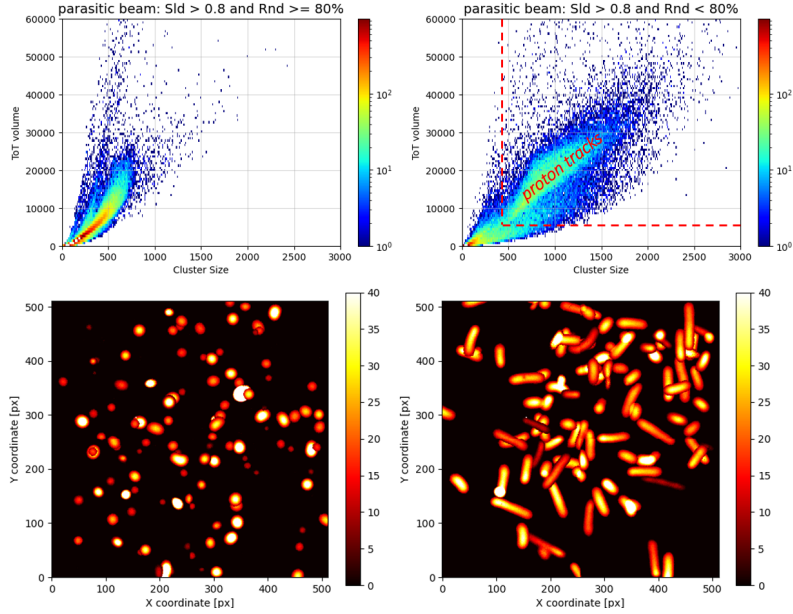


Figure 8: *Upward: 2D histogram plot of the ToT volume versus Cluster Size with roundness parameter lower and higher than 0.8, the proton region was further outlined in the second plot; Downward: the observed track morphology of tracks belonging to the two highlighted 2D populations.*

In this case, based on the MC simulations, it has been observed that these tracks come mainly from the neutron interaction on the mylar window. The long tracks at high energies can be ascribed to recoil protons produced on mylar, while circular blobs come from the interaction of Carbon, Oxygen, and Aluminum ions. As can be observed, the contribution from these ions can be further discriminated. In order to identify all these ions, some laboratory tests and dedicated simulations are ongoing.

## 6 Measurements of $^{10}\text{B}$ superficial density with a Silicon Timepix3 Quad Detector

In the field of Boron Neutron Capture Therapy (BNCT), the Knowledge of  $^{10}\text{B}$  content in biological samples is of fundamental importance because it is correlated to the effectiveness of the treatment. In particular, it is important to evaluate the  $^{10}\text{B}$  concentration and its spatial distribution inside cancerous tissues. Usually, two methods are used: the  $\alpha$  Spectrometry [10] to measure the concentration and Neutron Autoradiography [11] to image its spatial distribution. However, these two techniques must be applied separately, while autoradiography is laborious and involves the destruction of the analyzed sample. In this last year, it has been proposed a Silicon Timepix quad detector that is able to perform simultaneously the  $\alpha$  Spectrometry required to measure the concentration of  $^{10}\text{B}$  and imaging of the spatial distribution of this concentration. The used Timepix1 quad was a pixelated detector covering an area of  $28 \times 28 \text{ mm}^2$  with a matrix of  $512 \times 512$  square pixels, having a pitch of  $55 \mu\text{m}$ . It can acquire in three different modes with respect to the incident particles: counting, charge (ToT mode), or time of arrival (ToA). The fist tests have been



performed at the LENA reactor in Pavia and provided satisfying results. We refer to the degree thesis of A. Feruglio [12] for further details. After these first encouraging results, the detection system has been improved using a 100  $\mu\text{m}$  silicon Timepix3 quad having the same pixel configuration of Timepix1 quad but with a reduction of the background thanks to the removal of the underlying support (fig. 9a). In addition, it provides also an optimization of acquisition respect to its predecessor. Compared to Timepix1, TPX3 can work simultaneously in counting, charge and time, while data are transferred in sequence pixel by pixel without integration (data-driven-based). This last functionality allowed us to avoid the charge overlapping problem that affected measures with Timepix1 quad. The experimental set-up included a polypropylene mask with a sample holder at the center as shown in fig. 9b.

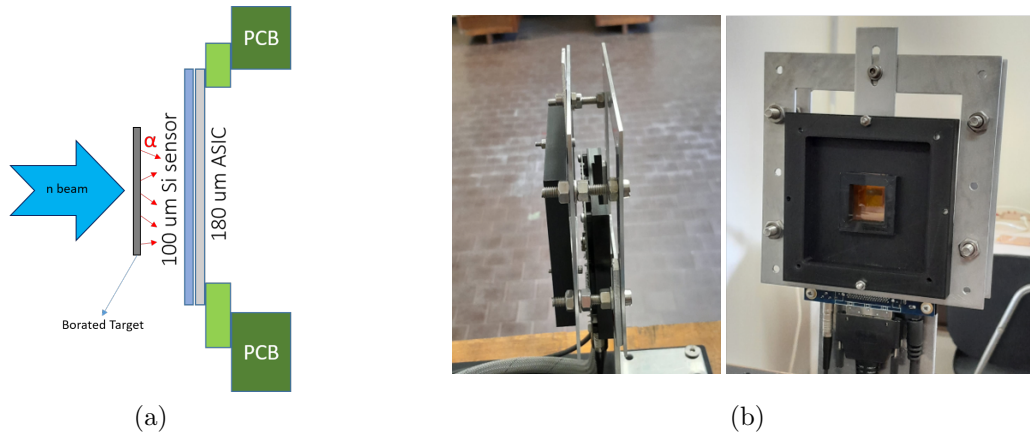


Figure 9: a) The layout of the experimental set-up with the new TPX3 quad detector, there is no PCB board on back of the quad; b) a photo of the experimental set-up, It is possible to see the polypropylene mask where samples can be mounted.

The experiment aimed to realize the Boron imaging concentration on two types of samples: Aluminum sheets deposited with 1  $\mu\text{m}$  of  $\text{B}_4\text{C}$  with a concentration of  $10^{18}$  Boron atoms/ $\text{cm}^2$  and NIST silicon sample with  $10^{15}$  Boron atoms/ $\text{cm}^2$ . These samples were placed on the holed of the polypropylene mask at a distance of about 2-3 mm from the Timepix3 quad surface. Then they were irradiated by a neutron beam with a diameter of 5 cm. The LENA reactor provides a thermal neutron energy spectrum peaked at 25 mV and was operated at different powers (from 1 to 250 kW) in order to change the neutron flux. At the maximum power of 250 kW, the estimated neutron flux on the sample is about  $6.2 \times 10^6$  neutrons/ $\text{cm}^2 \cdot \text{s}$  and scales proportionally with power. TPX3 quad acquires not only the  $\alpha$  particles produced by the reaction  $^{10}\text{B}(n,\alpha)^7\text{Li}$  but also the background due especially to the gamma activation of the surrounding materials. Then a track discrimination must be performed to identify the alpha tracks and realize the corresponding image of  $^{10}\text{B}$  deposition. Fig. 10 shows the images obtained with a  $\text{B}_4\text{C}$  target and a NIST sample after 10 minutes of irradiation with the reactor working at 25 kW.

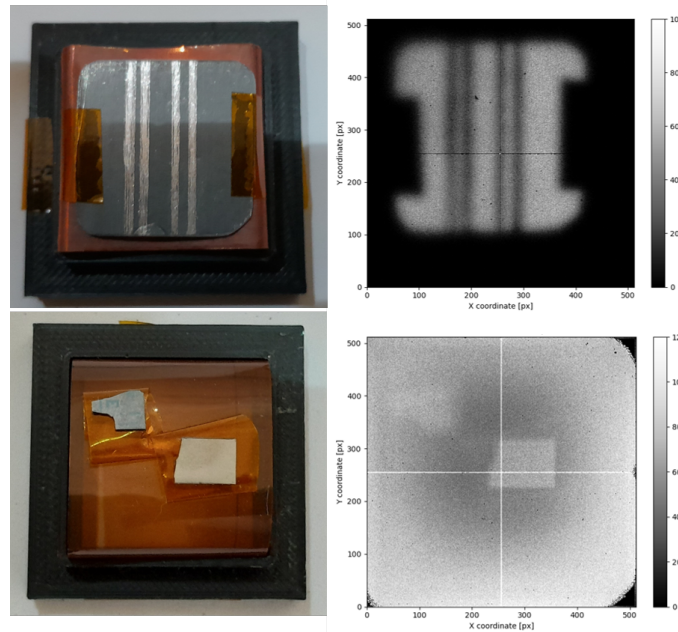


Figure 10: *Upwards: a sample of Aluminum sheet with 1  $\mu\text{m}$  of  $B_4C$  deposition and the image obtained after selecting the centroids of  $\alpha$  tracks; Downwards: two NIST samples of Silicon sheets with  $^{10}\text{B}$  implantation and the image obtained after selecting the centroids of  $\alpha$  tracks.*

Both images have been obtained plotting the centroids of tracks selected by applying specific cuts on the morphological parameters and charge. This procedure aimed to identify tracks due to  $\alpha$  particles. In particular, the image of the NIST sample has been obtained with a cut in energy of 0.8 MeV. This last result is very important because the concentration is similar to that used on tissues for BNCT treatments. At the moment, data analysis is in progress and will be integrated with MC Fluka simulations to identify the main contributions to better reconstruct the image and measure the relative concentrations.

## 7 List of Conference Talks and Posters by LNF Authors in Year 2023

1. A. Tamburrino, Il rivelatore Timepix3 per la misura di neutroni termici, XXXIX Congresso Nazionale Airp, Cagliari, 27–29 Settembre 2023
2. S. Tosi, A bridge to the end of the life of a star, STARS (Across the Universe) meeting, Napoli, 16-20 Ottobre 2023

## 8 Publications

List of papers published by Frascati n\_TOF members in 2023:

1. A. Tamburrino, G. Claps, G.M. Contessa, A. Pietropaolo, F. Cordella, V. De Leo, R.M. Montereali, M.A. Vincenti, V. Nigro, R. Gatto, D. Pacella, Thermal neutron detection by means of Timepix3, *Eur. Phys. J. Plus*, vol. 138, no. 11, p. 988, 2023, doi: 10.1140/epjp/s13360-023-04583-0
2. F. Cordella, M. Cappelli, M. Ciotti, G. Claps, V. De Leo, C. Mazzotta, D. Pacella, A. Tamburrino, F. Panza, Genetic algorithm for multilayer shield optimization with a custom parallel computing architecture, *Eur. Phys. J. Plus*, 2024, doi: 10.1140/epjp/s13360-023-04842-0
3. V. De Leo, G. Claps, F. Cordella, G. Cristoforetti, L.A. Gizzi, P. Koester, D. Pacella, A. Tamburrino, "Combined Spectroscopy System Utilizing Gas Electron Multiplier and Timepix3 Technology for Laser Plasma Experiments," *Condens. Matter*, vol. 8, no. 4, 2023, doi: 10.3390/condmat8040098.
4. S. Cesaroni, F. Bombarda, S. Bollanti, C. Cianfarani, G. Claps, F. Cordella, F. Flora, M. Marinelli, L. Mezi, E. Milani, D. Murra, D. Pacella, S. Palomba, C. Verona, G. Veron-Rinati, Conceptual design of CVD diamond tomography systems for fusion devices, *Fusion Engineering and Design*, Volume 197 December 2023, Article number 114037, doi: 10.1016/j.fusengdes.2023.114037

## References

1. T. Poikela et al. 2014. Timepix3: a 65k channel hybrid pixel readout chip with simultaneous ToA/ToT and sparse readout. *J. Instrum.* 9, C05013 (2014)
2. G. Claps, F. Murtas, L. Foggetta, C. Di Giulio, J. Alozy and G. Cavoto, Diamondpix: A CVD diamond detector with timepix3 chip interface, *IEEE Trans. Nucl. Sci.* 65 (2018) 2743
3. A. Tamburrino, PhD Thesis on "Characterization of a new pixelated diamond detector for fast neutron diagnostics on fusion reactors", Sapienza University of Rome (2024)
4. D.S. McGregor, M.D. Hammig, Y.-H. Yang, H.K. Gersch, R.T. Klann, Design considerations for thin film coated semiconductor thermal neutron detectors-i: basics regarding alpha particle emitting neutron reactive films. *Nucl. Instrum. Methods Phys. Res. A* (2003). [https://doi.org/10.1016/S0168-9002\(02\)02078-8](https://doi.org/10.1016/S0168-9002(02)02078-8)
5. L. Cosentino, F. Murtas et al., Proposal to the ISOLDE and Neutron Time-of-Flight Committee, Measurement of (n,cp) reactions in EAR1 and EAR2 for characterization and validation of new detection systems and techniques, CERN-INTC-2022-019/INTC-P-629 (2022)
6. Falk Herwig 2005, *Annual Review of Astronomy & Astrophysics*, vol. 43, Issue 1, pp.435-479

- 7 . Barbagallo et al., (n,cp) reactions study at the n\_TOF facility at CERN: results for the Cosmological Lithium problem, CERN Proc. 1 (2019) pp.259-264
- 8 . F. Murtas, The GEMPix detector, Rad. Meas. 138, 106421 (2020)
- 9 . X. Llopart et al., Timepix, a 65k programmable pixel readout chip for arrival time, energy and/or photon counting measurements. Nucl. Instr. Meth. A 581, 485 (2007)
- 10 . S. Bortolussi e S. Altieri. "Boron concentration measurement in biological tissues by charged particle spectrometry". In: Radiation and Environmental Biophysics 52 (4 2013). DOI: 10.1007/s00411-013-0480-y
- 11 . S. Altieri et al. "Neutron autoradiography imaging of selective boron uptake in human metastatic tumors". In: Applied Radiation and Isotopes 66 (12 2008). DOI: 10.1016/j.apradiso.2008.05.007
- 12 . A. Feruglio, Degree Thesis on "Misura della Concentrazione e della Distribuzione del  $^{10}\text{B}$  per la Boron Neutron Capture Therapy con Rivelatori Timepix", Pisa University (2022)